

Evidence for Kosterlitz-Thouless-type orientational ordering of CF₃Br monolayers physisorbed on graphite

S. Faßbender, M. Enderle, and K. Knorr

Technische Physik, Universität des Saarlandes, 66041 Saarbrücken, Germany

J. D. Noh and H. Rieger

Theoretische Physik, Universität des Saarlandes, 66041 Saarbrücken, Germany

(Received 22 October 2001; published 4 April 2002)

Monolayers of the halomethane CF₃Br adsorbed on graphite have been investigated by x-ray diffraction. The layers crystallize in a commensurate triangular lattice. On cooling they approach a three-sublattice antiferroelectric pattern of the in-plane components of the dipole moments. The ordering is not consistent with a conventional phase transition, but points to Kosterlitz-Thouless behavior. It is argued that the transition is described by a six-state clock model on a triangular lattice with antiferromagnetic nearest-neighbor interactions which is studied with Monte Carlo simulations. A finite-size scaling analysis shows that the ordering transition is indeed in the KT universality class.

DOI: 10.1103/PhysRevB.65.165411

PACS number(s): 68.35.Rh, 61.10.Nz, 64.60.Cn

Two-dimensional (2D) systems cannot show long-range order by breaking a continuous symmetry at any finite temperature T . Nevertheless Kosterlitz and Thouless (KT) demonstrated that a 2D XY ferromagnet with nearest-neighbor interaction and equivalently a planar rotator exhibit a phase transition from an ordered phase with an algebraic decay of the spin correlations to a disordered phase via the unbinding of vortex-antivortex pairs.¹

The KT concept has been applied successfully to the onset of superfluidity^{2,3} and of superconductivity⁴ in thin films and two-dimensional melting.⁵ An application to layered magnetic systems with large ratios of intra- and interlayer exchange appears to be more direct, but here the KT transition is masked by the transition to 3D behavior.⁶ In the present article we present x-ray diffraction data on CF₃Br monolayers physisorbed on graphite and present evidence that the orientational *pseudospin* ordering is of the KT type.

Physisorbed monolayers are indeed good approximations to 2D systems, as evidenced by the fact that phase transitions occurring in such layers can be often described by the 2D versions of elementary models of statistical mechanics such as the Ising or three-state Potts model.⁷⁻⁹

The halomethane CF₃Br is a prolate C_{3v} molecule with a fixed dipole moment of about 0.5 D pointing along the three-fold axis parallel to the C-Br bond. Monolayers have been adsorbed on exfoliated graphite and investigated by x-ray powder diffraction. The coverage ρ , temperature T phase diagram is rather complex.^{10,11} Here we concentrate on a coverage which is representative of the extended monolayer regime in which the monolayer lattice is commensurate with the graphite lattice. Diffraction patterns are shown in Fig. 1. The peaks of the patterns have been analyzed for position, intensity, and coherence length, as has been described elsewhere.^{9,11} The commensurate layer melts around 105 K.¹² In the 2D solid state, the diffraction pattern is dominated by the principal Bragg reflection of the commensurate, triangular 2×2 lattice at $Q_p = 1.475 \text{ \AA}^{-1}$. Just below the melting temperature, this peak is in fact the only one visible. Down

to the lowest T , the peak position is independent of T , as imposed by the commensurability with the substrate. The peak width yields a coherence length of about 180 \AA throughout the 2D solid state which compares well with the average lateral size of the crystallites of exfoliated graphite usually quoted in the literature. The 2×2 structure has been also observed for monolayers of CF₄ (Ref. 13), CF₃Cl (Ref. 14), C₂F₆ (Ref. 15) on graphite. These molecules and CF₃Br have threefold symmetry and the CF₃ group in common. Hence it is plausible to assume that CF₃Br stands on the substrate, presumably with the F₃ tripod down. An isolated CF₃Br would prefer to lie flat on the substrate, but definitely the 2×2 mesh is too tight to accommodate the molecules in this orientation. On the other hand, steric considerations suggest that the lateral 2×2 packing of perpendicular molecules can tolerate tilt angles of the molecular axis up to 30° with respect to the substrate normal. A tilt is equivalent to a non-zero in-plane component of the dipole moment. We regard this component as pseudospin S_i . In this sense the 2×2 state is disordered with a zero time average of every S_i and is

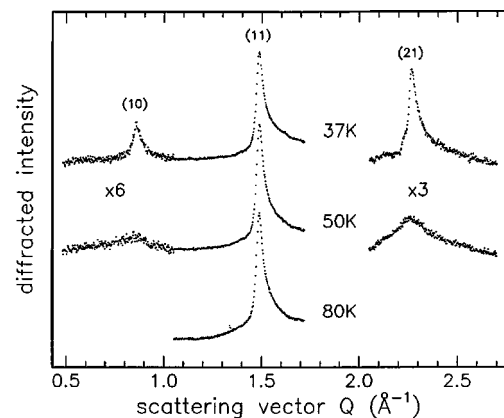


FIG. 1. Diffraction patterns of solid monolayers of CF₃Br on graphite ($\rho = 1.08$). The (hk) indices refer to the $2\sqrt{3} \times 2\sqrt{3}$ superlattice. The blind region is due to the strong (002) reflection of the graphite substrate.

stabilized at higher T by a libration and/or a precession of the molecular axis about the substrate normal.

On cooling, two additional features develop in the diffraction pattern which finally, below 40 K, can be regarded as Bragg peaks at $Q=0.851 \text{ \AA}^{-1}$ and 2.253 \AA^{-1} . They are easily identified as superlattice reflections brought forth by a tripling of the 2D mesh leading to a $2\sqrt{3} \times 2\sqrt{3}$ commensurate hexagonal lattice. The (hk) indices of Fig. 1 refer to this superlattice. The (20) reflection, which should occur at 1.703 \AA^{-1} , is absent. Below 40 K, the coherence length derived from the width of the superlattice reflections is again 180 \AA and is thus imposed by the substrate. The global structure of the low-temperature state must be consistent with the hexagonal plane group $p3$ with three molecules in the supercell. Regarding the molecules as rigid, there are five positional parameters: namely, the translational coordinates x, y and the three Eulerian angles of one molecule. The low number of reflections does not allow a rigorous determination of these parameters; nevertheless, one can make some semi-quantitative statements. A perpendicular orientation of the molecules in combination with a staggered azimuthal angle of the CF_3 group about the substrate normal is not sufficient to explain the superlattice intensities. The cell tripling must involve tilts of the molecular axes away from the perpendicular direction, presumably in combination with slight displacements of the molecule centers out of the original positions. A satisfactory agreement of measured and calculated intensities [including the accidental absence of the (20) reflection] is obtained with tilts of about 20° pointing toward a next neighbor such that the pseudospins form an antiferro-“magnetic” 120° Neel pattern on a 2D triangular lattice.

In case of a conventional order-disorder transition, the integrated intensities of the superlattice reflections would be a measure of the order parameter and should hence vanish when approaching the critical temperature from below. (See Ref. 9 for such a transition for $\text{C}_2\text{F}_5\text{Cl}$ on graphite.) This is, however, not what is observed in the experiment on CF_3Br monolayers. On heating the superlattice peaks broaden while keeping approximately their integral intensity until they are finally lost in the background. The temperature evolution of the (21) reflection is shown in Fig. 2 together with fits of a theoretical profile. The T dependence of the coherence length ξ as determined from the intrinsic width of this peak is shown in Fig. 3. The solid line of this figure is a fit of the KT expression

$$\xi = A \exp[B(T/T_K - 1)^{-1/2}] \quad (1)$$

to the data for $T > 40 \text{ K}$. The fit parameters are $A = 9 \pm 2 \text{ \AA}$, $B = 1.5 \pm 0.4$, and $T_K = 30 \pm 3 \text{ K}$. Note that the value of A is reasonably close to the lattice parameter of the 2D mesh. Thus ξ is expected to diverge at a KT critical temperature T_K of about 30 K, but the growth of the correlated regions is interrupted when ξ reaches the size of the graphite crystallites. This happens at about 40 K.

Given the scatter of the data points of Fig. 3, it is clear that fits with power laws $\xi \propto (T/T_C - 1)^{-\nu}$ are likewise possible. We do think, however, that an interpretation of the intensity between 40 K and 55 K in terms of conventional

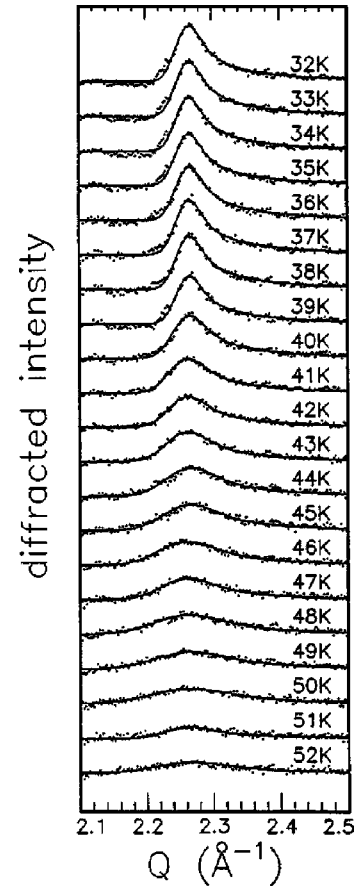


FIG. 2. The temperature evolution of the (21) superlattice reflection.

critical diffuse scattering, $T > T_C$, is not meaningful, because of the absence of any critical T dependence of the integrated intensities and because the diffuse scattering would be presumably far below the detection limit in x-ray or neutron diffraction studies on adsorbed monolayers on exfoliated graphite. At least we do not know of any successful experiment of this type.

The heat capacity measurement also shows an indication of the phase transition.¹² Apart from the melting anomaly, the heat capacity of commensurate CF_3Br monolayers shows an

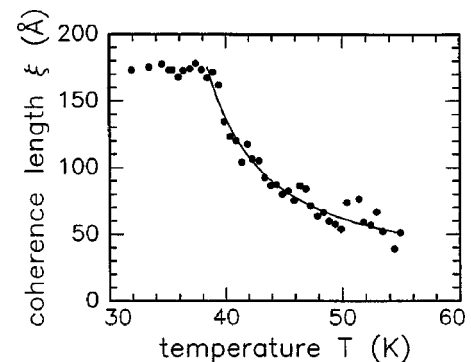


FIG. 3. The temperature dependence of the coherence length of the antiferroelectric correlations, as derived from the intrinsic width of the (21) reflection.

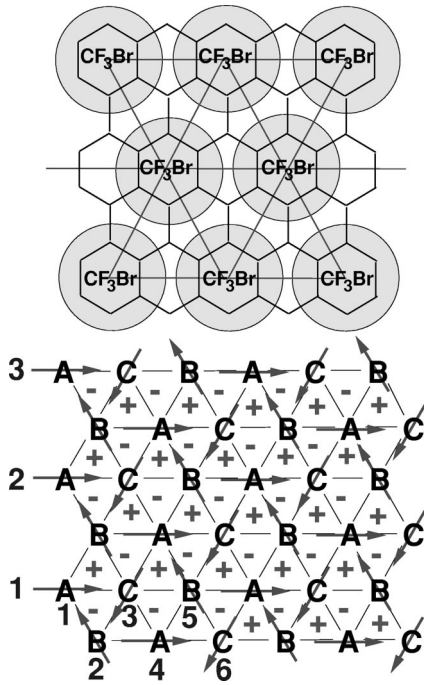


FIG. 4. Top: the spatial arrangement of the CF_3Br molecules on the underlying hexagonal graphite surface in the 2×2 structure that is present below 105 K. The resulting trigonal lattice is also shown. Bottom: a triangular lattice of size 12×3 with the six-state clock spins indicated as arrows representing the six preferred directions of the CF_3Br dipolar moments. The arrow configuration shown is one of the 12 ground states by which the lattice sites are separated into three A, B, and C sublattices. The helicity for each elementary triangle corresponding to this ground state is also indicated by + and -.

anomaly extending from 35 K to 40 K which is just the T range where ξ saturates. However, it does not allow a quantitative analysis of the critical scaling behavior since the anomaly is very weak.

Do CF_3Br monolayers meet the theoretical requirements for a KT transition? Clearly the pseudospin correlations are bound to a plane; thus, the system is 2D with respect to the relevant degrees of freedom at the phase transition. The pseudospin is presumably not a strictly isotropic planar rotator but experiences a crystal field which breaks the continuous azimuthal symmetry. It has been shown, however, that — at least for the planar XY ferromagnet — the KT behavior is stable with respect to small crystal fields of sixfold symmetry.¹⁶ The site symmetry of the monolayers is indeed sixfold, but the ordered structure approached is not ferro- but antiferroelectric. Antiferro-type ordering on a triangular lattice is affected by frustration with the consequence that the helicity, a discrete twofold symmetry, enters into the problem. The order-disorder transition is then described by a confluence of the Ising and KT universality classes^{17,18} with an Ising-type anomaly of the specific heat, but the spin correlations of the disordered phase still follow the KT form of $\xi(T)$ as we will demonstrate now.

From the above considerations follows that the pseudospins formed by the CF_3Br dipoles are arranged on a triangular lattice, interact antiferromagnetically with nearest

neighbors,¹⁹ and have six preferred orientations described by an azimuthal angle θ .²⁰ Hence the model that captures the *universal* features of the orientational ordering transition (i.e., those that are independent of the microscopic details of the interactions between the molecules) should be the antiferromagnetic six-state clock model on a 2D $N=L_x \times L_y$ triangular lattice (see Fig. 4). The six-state clock spin is a planar spin pointing toward discrete six directions: $\mathbf{S} = (\cos \theta, \sin \theta)$ with $\theta = 2\pi n/6$ ($n=0,1,\dots,5$). The Hamiltonian of this model reads

$$\mathcal{H} = 2J \sum_{\langle i,j \rangle} \cos(\theta_i - \theta_j), \quad (2)$$

where the sum is over nearest-neighbor site pairs $\langle i,j \rangle$ and $J > 0$ is the antiferromagnetic coupling strength. The overall factor of 2 is introduced for computational convenience. It is a limiting case of an antiferromagnetic XY model with infinite anisotropy field $\cos p\theta$ ($p=6$).

The antiferromagnetic coupling on a triangular lattice induces a frustration. As a result the system has 12-fold degenerate ground states with three-sublattice structure. Global spin rotations by multiples of $2\pi/6$ and also an Ising-like transformation that inverts all helicities formed by the spins on elementary triangles (see Fig. 4) transform one ground state into another. Therefore the model possesses a C_6 (six-fold clock) $\times Z_2$ (Ising) symmetry and we expect that there are two phase transitions associated with the spontaneous breaking of the C_6 and Z_2 symmetry.

We performed extensive Monte Carlo simulations of the model (2) using conventional single spin-flip dynamics with up to 10^8 Monte Carlo steps per spin and lattice sizes up to 384×192 and studied its phase transition with a thorough finite-size scaling analysis. Here we focus on the breaking of the C_6 symmetry that is indicated by the x-ray diffraction experiments reported above; the details of the breaking of the

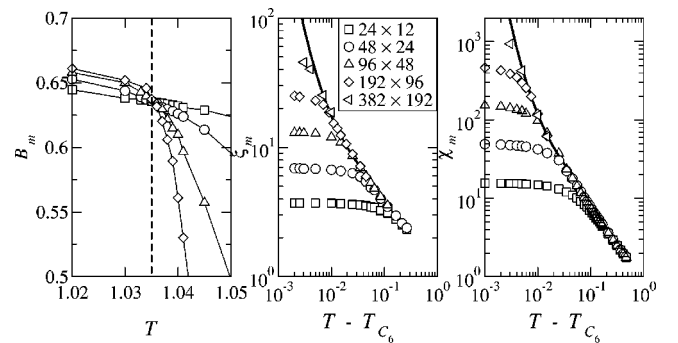


FIG. 5. Left: the Binder parameter B_m , Eq. (5), vs temperature for different system sizes. The intersection point of the different curves locates the critical temperature indicated by the broken line at $T_{C_6} = 1.035 \pm 0.0005$. Middle: the correlation length, Eq. (6), as a function of $T - T_{C_6}$ (with $T_{C_6} = 1.035$) in a log-log plot. Upwards curvature of the numerical data indicates already a faster-than-algebraic divergence. The solid line is a least-squares fit to the KT form (1). Right: the magnetic susceptibility with a fit to the expected KT form.

Z_2 symmetry (which happens at a slightly higher temperature and turns out to be in the Ising universality class) will be reported elsewhere.²¹

The order parameter for the C_6 symmetry is the sublattice magnetization

$$m_A = \frac{1}{N} \sum_{i \in A} \exp(i\theta_i), \quad (3)$$

where the sum runs over only sites in the A sublattice (m_B and m_C can be defined similarly). Analogously the spatial spin correlation function is defined as

$$C_m(r) = \left\langle \frac{3}{N} \sum_{i \in A} \cos(\theta_i - \theta_{i+r}) \right\rangle \quad (4)$$

and the susceptibility is given by $\chi_m = N \langle m_A^2 \rangle$.

The transition temperature is estimated using the dimensionless ratio of moments (or Binder parameter),

$$B_m = 1 - \frac{\langle m_A^4 \rangle}{3 \langle m_A^2 \rangle^2}, \quad (5)$$

which is shown in Fig. 5 and yields the critical temperature $T_{C_6} = 1.035 \pm 0.0005$. We extract the correlation length from the correlation function $C(r)$ defined in Eq. (4) via

$$\xi_m^2 = \frac{\sum_r r^2 C_m(r)}{\sum_r C_m(r)}. \quad (6)$$

Our data are shown in Fig. 5 in a log-log plot of $\xi_m(T)$ versus $T - T_{C_6}$ with T_{C_6} from above. They fit nicely to the KT form (1) with $A = 2.54$ and $B = 0.193$. Note that the non-universal number B differs significantly from the one for the experimental data, which is not unusual for microscopically different systems in the KT universality class (see, e.g., Ref. 22). The susceptibility, also shown in Fig. 5, follows the expected KT form $\chi_m = A' \exp[B'(T - T_{C_6})^{-1/2}]$, too. We also checked other quantities [like the decay of $C_m(r)$ at T_{C_6}] and found everything to be consistent with a KT scenario.

In summary, our measurements show that CF_3Br molecules physisorbed on graphite are arranged in a commensurate triangular lattice. On cooling, a Néel-type 120° pattern is approached. The growth of the critical correlations has been followed over a wide temperature range. It finally stops when the correlation length reaches the size of the substrate crystallites. The behavior is consistent with the KT scenario. An antiferromagnetic six-state clock model on a triangular lattice, which we studied numerically, describes the universal features of this ordering transition well.

This work has been supported by the Deutsche Forschungsgemeinschaft (Project No. Kn234/9 and SFB 277).

-
- ¹J. M. Kosterlitz and D. J. Thouless, *J. Phys. C* **6**, 1181 (1973); J. M. Kosterlitz, *ibid.* **7**, 1046 (1974).
- ²D. J. Bishop and J. D. Reppy, *Phys. Rev. Lett.* **40**, 1727 (1978).
- ³I. Rudnick, *Phys. Rev. Lett.* **40**, 1454 (1978).
- ⁴M. R. Beasley, J. E. Mooij, and T. P. Orlando, *Phys. Rev. Lett.* **42**, 1165 (1979).
- ⁵B. I. Halperin and D. R. Nelson, *Phys. Rev. Lett.* **41**, 121 (1978); D. R. Nelson and B. I. Halperin, *Phys. Rev. B* **19**, 2457 (1979).
- ⁶L. P. Regnault and J. Rossat-Mignod, in *Magnetic Properties of Layered Transition Metal Compounds*, edited by L. J. de Jongh (Kluwer Academic, Dordrecht, 1990), p. 271.
- ⁷M. Bretz, *Phys. Rev. Lett.* **38**, 501 (1977).
- ⁸Y. P. Feng and M. H. W. Chan, *Phys. Rev. Lett.* **71**, 3822 (1993).
- ⁹S. Fassbender, C. Steimer, D. Arndt, and K. Knorr, *Phys. Rev. Lett.* **75**, 2526 (1995); *Surf. Sci.* **388**, 201 (1997).
- ¹⁰E. Maus, Ph.D. thesis, Universität Mainz, 1991.
- ¹¹K. Knorr, *Phys. Rep.* **214**, 113 (1992).
- ¹²K. Knorr, S. Fassbender, A. Warken, and D. Arndt, *J. Low Temp. Phys.* **111**, 339 (1998).
- ¹³B. Crosset, C. Marti, P. Thorel, and H. J. Lauter, *J. Phys. (Paris)* **43**, 1659 (1982).
- ¹⁴W. Weimer, K. Knorr, and H. Wiechert, *Z. Phys. B: Condens. Matter* **73**, 235 (1988).
- ¹⁵D. Arndt, S. Fassbender, M. Enderle, and K. Knorr, *Phys. Rev. Lett.* **80**, 1686 (1998).
- ¹⁶J. V. José, L. P. Kadanoff, S. Kirkpatrick, and D. R. Nelson, *Phys. Rev. B* **16**, 1217 (1977).
- ¹⁷D. H. Lee, J. D. Jannopoulos, J. W. Negele, and D. P. Landau, *Phys. Rev. Lett.* **52**, 433 (1984); *Phys. Rev. B* **33**, 450 (1986).
- ¹⁸S. Lee and K.-C. Lee, *Phys. Rev. B* **49**, 15 184 (1994); P. Olsson, *Phys. Rev. Lett.* **75**, 2758 (1995); H. J. Xu and B. W. Southern, *J. Phys. A* **29**, L133 (1996).
- ¹⁹The character of the relevant orientation-dependent interactions of CF_3Br is not known, but a comparison of monolayers of several polar methane derivatives (Ref. 11) suggests that for CF_3Br the short-range anisotropic part of the intermolecular van der Waals force and hard-core repulsion are more important than the medium-range dipole-dipole interaction.
- ²⁰The polar orientation of the normal component of the dipole moments is not resolved by the x-ray diffraction data.
- ²¹J. D. Noh *et al.* (unpublished).
- ²²S. W. Pierson *et al.*, *Phys. Rev. B* **60**, 1309 (1999).